

Detection of breast cancer in mammography : a neural approach. I. detection of clustered microcalcifications.

Jacques G. DIAHI **, Alain Giron **, Christophe FROUGE *, Bernard FERTIL **
** INSERM (U 66), CHU Pitié Salpêtrière, 91 boulevard de l'Hôpital, 75634 Paris cedex 13,
France

* Service de Radiologie centrale CHU de Bicêtre, 94275 Kremlin Bicêtre, France.

Abstract

An automatic detection system of breast cancer is being developed in our laboratory. Clustered microcalcifications, stellate images, circumscribed opacities and asymetry of density are investigated. A set of artificial neural networks specialized in the detection of each abnormality, have been defined for this task. This paper present the specialist that performs the detection of clustered microcalcifications. It is a classical three-layer neural network, trained with the Back-Propagation algorithm. The mammogram is analysed by small portions extracted from the image scanned from the left to the right and from the top to the bottom. Success rate is 97 % for clustered microcalcifications regions and 95 % for areas without any microcalcifications.

Keywords : breast cancer, mammography, microcalcifications, classification, neural networks.

Résumé

Un système de détection automatique du cancer du sein est en cours de développement dans notre laboratoire. Les foyers de microcalcifications, les images stellaires, les opacités circonscrites et les asymétries de densité sont les anomalies considérées. Des réseaux de neurones artificiels, spécialisés chacun dans la détection d'une anomalie donnée, ont été définis pour cette tâche. Ce papier présente le module chargé de la détection des foyers de microcalcifications. C'est un réseau de neurones à trois couches, conçu avec l'algorithme de rétro-propagation. La mammographie est analysée de la gauche vers la droite et de haut en bas, à travers de petites portions. Le taux de succès est de 97 % pour les zones contenant des foyers de microcalcifications et de 95 % pour celles qui n'en contiennent pas.

Mots clés : cancer de sein, mammographie, microcalcifications, classification, réseaux de neurones.

1. Introduction

Breast cancer is one of the leading causes of cancer mortality in women, in developed countries. For example, approximately 26,000 new breast cancers per year are expected to be diagnosed in France. For this same country, there were 10,200 deaths due to breast cancer in 1990, corresponding to a basic mortality rate of 35.2 per 100,000 women. It presently accounts for 18,9% of all female cancer deaths [1].

Mammography is the only breast cancer detection technique presently available with proven efficacy. Mammograms screening by radiologists is a difficult task because of the low contrast, the subtlety and the small size of breast cancer features. A large amount of classical algorithms have been investigated for mammograms analyses [2, 3, 4, 5, 6]. Most of these algorithms offer a system that is designed to perform an automatic detection and/or classification of microcalcifications [2, 3, 4].

Artificial neural networks, which is a non-parametric new approach to information processing, have been intensively studied in the field of computer science, engineering, physics, neurology, biology and psychology, in the last ten years. Artificial neural networks models learn by experience, generalize from previous experiences to new ones, and can make decisions. But these networks are very known because of their ability to draw conclusions when presented with complex, "noisy", or partial information [7].

In the context of mammography, artificial neural networks have been applied to a variety of pattern-recognition tasks such as microcalcifications detection and specification (shape, size, type etc...) [7, 8, 9, 10] and have been shown to provide a potentially powerful classification tool for microcalcifications (benign / malignant) [8, 11, 12]. The other abnormalities such as stellate images, opacities or asymmetric densities are not very investigated.

A computer-aided diagnosis scheme, based on the expertise of several artificial neural networks specialists, is being developed. Each specialist is built in order to recognize a specified abnormality of breast cancer. A supervisor network give the final decision. This paper describe the realisation of the specialist concerned with the detection of clusters of microcalcifications.

2. The microcalcification specialist

2.1 Materials

The database was made of 200 mammograms of patients who underwent surgery for a local lesion suggestive of malignancy and 100 mammograms without any suspicious lesion. The mammograms were categorized into five groups : clusters of microcalcifications, stellate lesions, asymetry of density, circumscribed opacities and "normals". Mammograms were scanned with a Kodak DCS 420 camera, at a resolution

of 1524 x 1012 pixels (8 bits) and a 256 gray level dynamic range. Each digital image was about 1.5 Mb. The program was developed on a Macintosh platform, using VIP-C and THINK-C.

2.2 Methods

Digitized mammograms are used as input to the system for determining the presence of cancer signs, by finding the locations of detected suspicious abnormalities on the image itself. Rather than making a real segmentation of the detected abnormalities, the aim of the system is to point out and outline a suspicious area containing these abnormalities (see [9] for more information about the system architecture).

2.2.1 The mammogram scanning

The main purpose of the system is to analyse the mammogram by scanning the whole numerical image through small portions (called **vignettes** in the following sections). Given a vignette, the network tries to classify it as a clustered microcalcifications vignette or not. The classification is done with features extracted from the vignette (figures 1A and 1B). The specialist is a three-layer feedforward neural network.

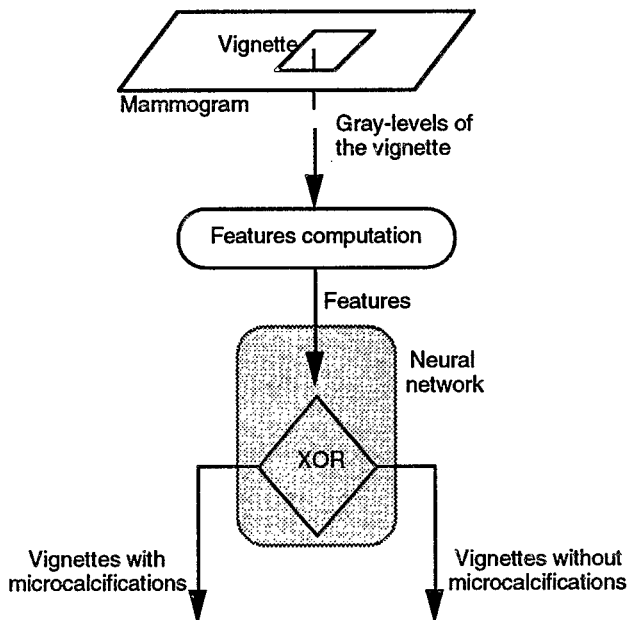


Figure 1A : the specialist general architecture

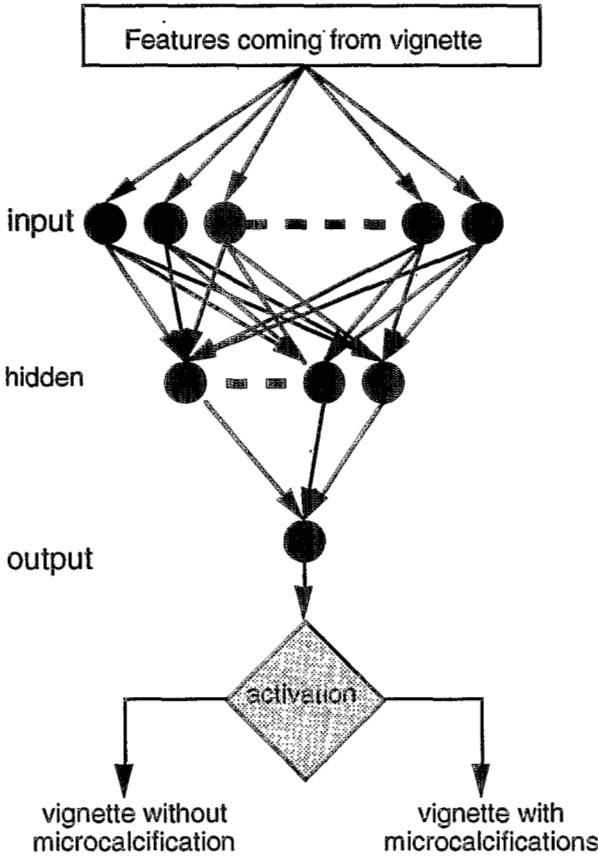


Figure 1B : the neural network architecture

2.2.2 The training data

Two sets of vignettes are used for the training process : one for the effective training (the learning set) and the other for stopping the training phase (the validation set), in order to avoid the network to be overtrained. This is done because an overtrained neural network may improve performance on the learning set, while predictions are degraded on the validation set (the system fails to generalize). In this study, the learning set is made of 434 vignettes (200 with microcalcifications and 234 without) and the validation one is made of 385 imagettes (175 with microcalcifications and 210 without). The vignettes containing microcalcifications are randomly placed on the abnormalities (figure 2).

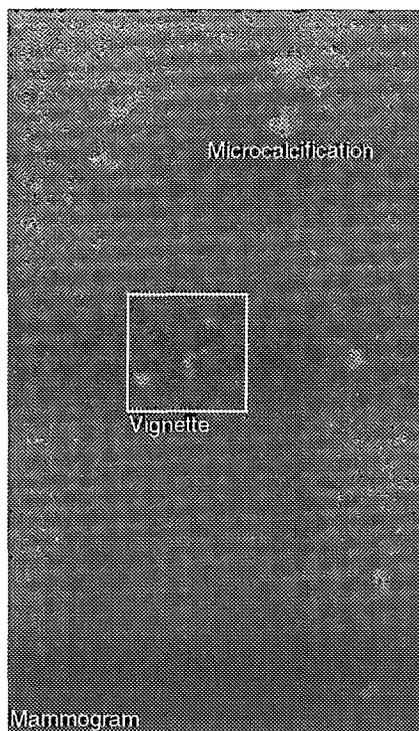


Figure 2: vignette representation

2.2.3 The features extraction

The network is trained on features calculated from vignettes of 32 x 32 pixels size. Since microcalcifications look like small textured structures with different shape and intensity, a transformation is applied to the vignette, in order to characterize the gray-level contrast between the microcalcifications and the local background. This contrast is given by the gray-level difference between two windows w_1 and w_2 . The window w_1 has a size close to microcalcifications and is designed to give their mean gray-level intensity. For this study w_1 is a window of 4 x 4 pixels size. The window w_2 is greater than w_1 which is centered and surrounded by it (figure 3). Window w_2 may give the local background mean gray-level intensity. A 12 x 12 pixels window is used for w_2 . This filter is applied to the whole vignette, scanned from the left to the right and from the top to the bottom, with a step set to the size of the window w_1 . Thus the transformed vignette (called T_v thereafter) is a 8 x 8 matrix of data. Each value of T_v is a difference between w_1 and w_2 at a corresponding scanning step.

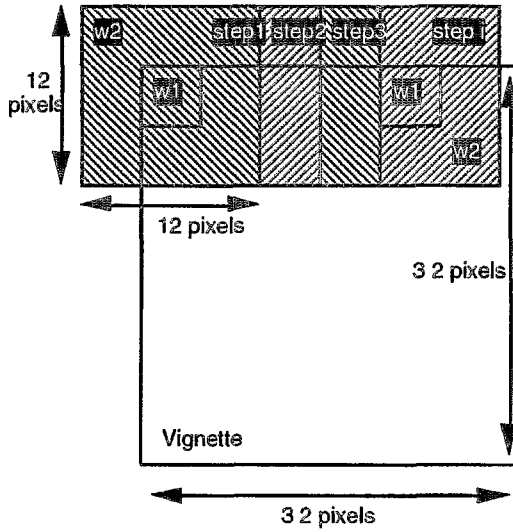


Figure 3: scanning vignettes with windows w1 and w2

After normalisation of T_v , four parameters are computed:

$$F1 = \frac{1}{\max} \sum_i \sum_j [T_v(i,j) - T_v(i,j+1)]^2 ; \quad (1)$$

$$F2 = \frac{1}{\max} \sum_i \sum_j T_v(i,j) \times \log T_v(i,j) ; \quad (2)$$

$$F3 = \frac{1}{\max} \sum_i \sum_j [T_v(i,j) - \text{moy}(T_v)]^2 ; \quad (3)$$

$$F4 = \frac{1}{\max} \sum_i \sum_j T_v(i,j)^2 ; \quad (4)$$

were :

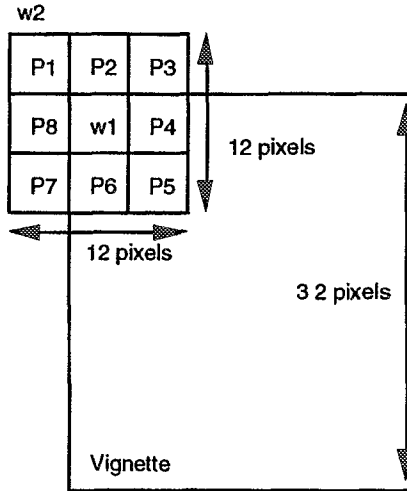
$$i \in [1, \max_i] \text{ and } j \in [1, \max_j] ;$$

$$\text{with } \max_i = \max_j = \frac{\text{size}_{\text{vignette}}}{\text{size}_{w1}} ;$$

$$\max = \max_i \times \max_j ;$$

$$\text{moy}(T_v) = \frac{1}{\max} \sum_i \sum_j T_v(i,j) ;$$

Another feature is used in order to take into account the local variation of the gray-level in the window w_2 . For this, the window w_2 is divided into 9 equal portions (figure 4).



Where : P_i is the mean of gray-level in portion P_i .

Figure 4: the 9 portions of window w_2 for feature F5

The mean of the gray-level is calculated on each portion. The feature F5 is then computed by summing the gray-level difference of two consecutived portions. The central portion which is equal to window w_1 is not considered in this feature. Feature F5 is given by:

$$F5 = \sum_i |P_i - P_{i+1}| ; \tag{5}$$

To obtain meaningful interpretation of the vignette informations, it is also important to take the overall gray-level distribution of the vignette into account. This task is carried out by the last feature F6 witch gives the mean of the gray-levels of the vignette. Thus feature F6 is obtained by:

$$F6 = \frac{1}{\text{size}_{\text{vignette}}^2} \sum \text{gray_level}_{\text{vignette}} ; \tag{6}$$

2.2.4 The neural network specification

A three-layer neural network architecture is selected for this specialist. 6 units are used for the input layer, 2 units for the hidden layer and 1 unit for the output layer. The network is trained to give 0.1 output value for the vignettes without microcalcification and 0.9 output value for vignettes with microcalcifications. In this study, the network decision threshold is set to 0.5. Thus if the output value of the specialist is lower than 0.5, the vignette is considered to be without microcalcification. But an output value higher than 0.5 indicates the presence of a cluster of microcalcifications.

3. The results

The performance of the network was evaluated using a test data set. It is made of vignettes randomly chosen on the mammograms. These vignettes were neither present in the learning set, nor in the validation set. Tables 1, 2 and 3 present the performances on the learning, the validation and the test set respectively.

Table 1: The network performance on the learning set

		Network expert		
		W	W/O	
Human expert	W	190	10	200
	W/O	7	227	234
		197	237	Total

Table 2 : The network performance on the validation set

		Network expert		
		W	W/O	
Human expert	W	170	5	175
	W/O	10	200	210
		180	205	Total

Table 3 : The network performance on the test set

		Network expert		
		W	W/O	
Human expert	W	98	2	100
	W/O	3	97	100
		101	99	Total

Where : W is for "with microcalcifications" and W/O for "without microcalcification"

The network performs a good classification for the vignettes of the three sets (96% for both learning and validation sets and 97,5% for the test set). These results of total correct classification rates, shows that the neural network is able to remember the vignettes that were used for its training. The second information get from these results is that the network is able to recognize and classify new vignettes it has never seen before. The selected features seems to characterize microcalcifications in such a way that, using our neural network, it is possible to identify and make decision between vignettes with or without microcalcifications, with a operative level of confidence. Actual results are better than those we obtained with the cooccurrence matrix method presented in [9].

The network performance was also evaluated on 23 entire mammograms. The detection and location of clusters of microcalcifications was about 100% on these mammograms (all clusters of microcalcifications were detected and located). Figures 4A, 4B, 4C and 4D shows the network performance on four kinds of mammogram. Figures 4A, 4B and 4C presents three mammograms with microcalcifications. Figure 4D presents a mammogram without microcalcification.

4. Discussion and future directions

The system accuracy is good in both easy and difficult to diagnose cases (high background gray-level with poor contrast between the background and very small microcalcifications). Comparing our results with the classification rates of the literature (74% in the best case in [12] and 85% at least in [7]), our system is really interesting. Nevertheless, it should be noted that classification results are sensitive to the selection of learning and test sets. More difficult cases will be added to the learning set for the network training phase, in order to make it more powerful and robust. This specialist is actually being tested on a more larger database of mammograms for validation of the detection and recognition of vignettes, when scanning the entire mammogram.

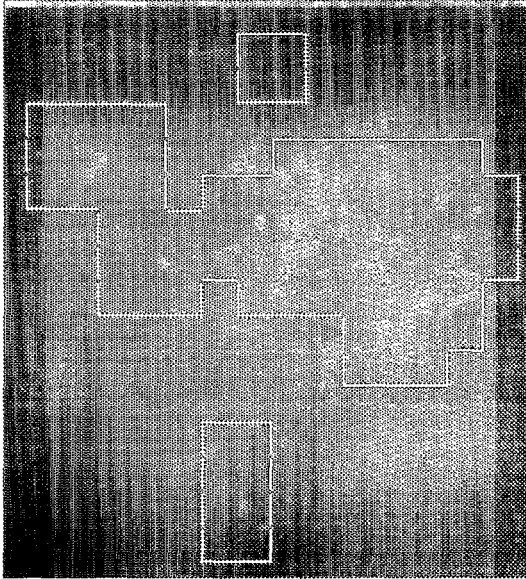


Figure 4A

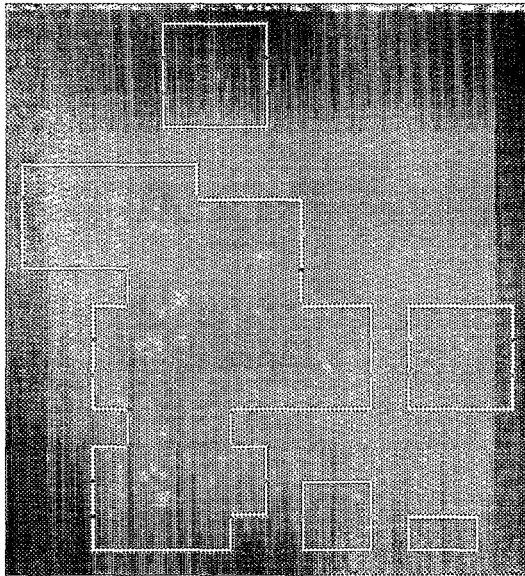


Figure 4B

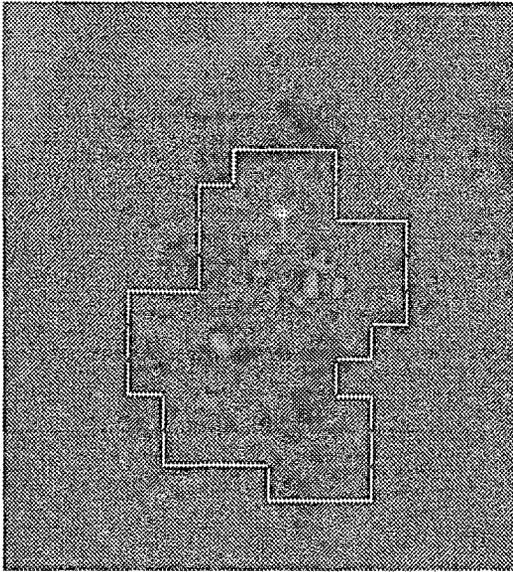


Figure 4C

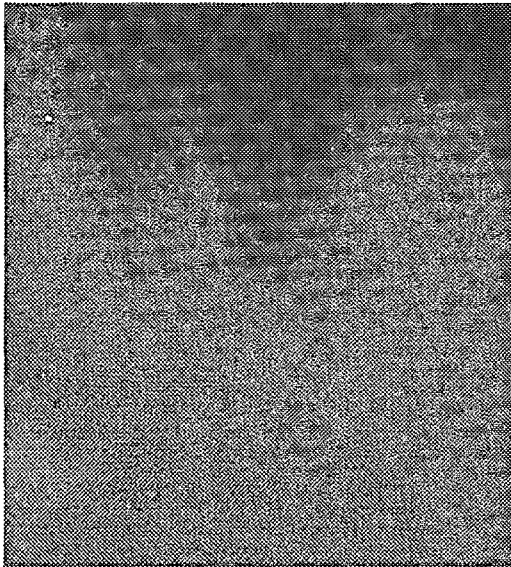


Figure 4D

Figure 4: four kinds of mammogram tested by the specialist

References

1. C. Hill, S. Koscielny, F. Doyon and E. Benhamou, Évolution de la mortalité par cancer en France 1950-1990, Statistiques de santé, Éditions INSERM (1993).
2. E. Kahn, A. Gavaille, J. Masselot, F. Bertin and J. Genin, Computer Analysis of Breast Microcalcifications in Mammographic Image, Computer Assisted Radiology, Berlin, pp. 729-733, (1987).
3. H. P. Chan, K. Doi, C. J. Vyborny, K. L. Lam and R. A. Schmidt, Computer-Aided Detection of Microcalcifications in Mammograms - Methodology and Preliminary Clinical Study, Invest. Radiol. No 23, pp. 664-671 (1988).
4. D. H. Davies, D. R. Dance and C. H. Jones, Automatic Detection of Microcalcifications in Digital Mammograms using Local Area Thresholding Techniques, SPIE Medical Imaging No 1092, pp. 153-159 (1989).
5. R. Highnam, M. Brady and B. Shepstone, A representation for mammographic image processing, First international Conference, CVRMed'95, Nice, France, April 1995, Lecture Notes in Computer Science, Springer Verlag No 905, pp. 365-371 (1995).
6. N. Cerneaz and M. Brady, Finding Curvilinear structures in mammograms, First international Conference, CVRMed'95, Nice, France, April 1995, Lecture Notes in Computer Science, Springer Verlag No 905, pp. 372-382 (1995).
7. Y. Wu, M. L. Giger, K. Doi, C. E. Metz, R. M. Nishikawa, C. J. Vyborny and R. A. Schmidt, Application of artificial neural networks in mammography for the diagnosis of breast cancer, SPIE No 1778, pp. 19-27 (1992).
8. L. Shen, R. M. Rangayyan and J. E. L. Desautels, An automatic detection and classification system for calcifications in mammograms, SPIE No 1905, pp. 799-805 (1993).
9. J. G. Diahi, C. Frouge and B. Fertil, Artificial neural networks in mammography for the diagnosis of breast cancer. I. detection of clustered microcalcifications, Conference on Neural Networks and their Applications, Marseilles, France, March 1996, Neurap'95/96, pp. 259-264 (1996).
10. R. M. Carmona, F. I. Pico, J. M. Chamizo and F. E. Ruiz, Automatic detection system of microcalcifications in mammograms. Neural modeling, The 9th Scandinavian Conference on Image Analysis, Uppsala, Sweden, June 1995, pp. 1207-1214 (1995).
11. S. Désarnaud and A. Strauss, Classification de microcalcifications par réseaux de neurones, XXVIème Journées de Statistique, Université de Neuchâtel, pp. 252-255 (1994).
12. A. PA Dhawan, Y. Chitre and M. Moskowitz, Artificial neural network based classification of mammographic microcalcifications using image structure features, SPIE No 1905, pp. 820-831 (1993).